Spin pumping and interlayer exchange coupling through palladium

D. L. R. Santos, P. Venezuela, R. B. Muniz, and A. T. Costa[*]

Instituto de Física, Universidade Federal Fluminense, 24210-346 Niterói, RJ, Brazil
(Received 22 May 2013; revised manuscript received 24 July 2013; published 26 August 2013)

The magnetic behavior of ultrathin ferromagnetic films deposited on substrates is strongly affected by the properties of the substrate. We investigate the spin pumping rate, interlayer exchange coupling, and dynamic exchange coupling between ultrathin ferromagnetic films through palladium, a nonmagnetic substrate that displays strong Stoner enhancement. We find that the interlayer exchange coupling, both in the static and dynamic versions, is qualitatively affected by the electron-electron interaction within the substrate. For instance, the oscillatory behavior that is a hallmark property of the RKKY exchange coupling is strongly suppressed by the induced moment in Pd. Although the spin pumping rate of ferromagnetic films atop palladium is only mildly changed by the electron-electron interaction in Pd, the change is large enough to be detected experimentally. The qualitative aspects of our results for palladium are expected to remain valid for any nonmagnetic substrate where Coulomb repulsion is large.

I. INTRODUCTION

Palladium is a fascinating material. In bulk form it is nonmagnetic, but it is on the brink of becoming ferromagnetic: The product of its paramagnetic density of states at the Fermi level $\rho(E_F)$ by the intra-atomic effective Coulomb interaction U is very close to the critical value of 1. The bulk conductivity as a function of temperature displays a T^2 contribution due to scattering by spin fluctuations that dominates the contribution from scattering by phonons at low $T < 10$ K. Adding Ni impurities to bulk Pd in concentrations smaller than 2% increase dramatically the effect of spin fluctuations on electronic transport: The coefficient of the T^2 term in the conductivity is amplified by a factor of 10.[1]

These remarkable properties indicate that Pd is a nonmagnetic material where the effects of electron-electron interactions are strong enough to be observed experimentally. In fact, direct observation of paramagnons in bulk Pd have been reported very recently.[2]

Palladium is still a challenge to our most successful theory for the electronic structure of materials. Some implementations of DFT predict bulk Pd to be magnetic and it is usually necessary to tune the lattice constant used in the calculations to obtain nonmagnetic bulk Pd.[3]

The importance of nonmagnetic substrates in determining the spin dynamics of adsorbed ultrathin films and adatoms has been demonstrated unequivocally in recent years. Excitation energies and lifetimes may be strongly affected by the hybridization between magnetic entities' and substrates' electronic states. Nice examples are provided by ultrathin Fe layers on W(110), where the strong spin-orbit coupling in W induces a large anisotropy and a strong Dzyaloshinskii-Moryia coupling between Fe magnetic moments,[4,5] and by Fe adatoms on Cu(111)[6] and Ag(111),[7] where the hybridization with the substrate strongly dampens the spin excitations and produces large shifts in their energies compared to isolated atoms.

The effects of Pd's large Stoner enhancement have been thoroughly studied in the past. However, there seems to be relatively few studies exploring the effects of electron-electron interaction in Pd on interlayer exchange coupling or spin pumping. One of these studies[8] has shown that Pd may serve as a good sink for spin currents emanated from ferromagnetic materials. There it is suggested that the absorption of spin current is facilitated by the enhanced spin fluctuations in Pd.

Interlayer exchange coupling (IEC) received enormous attention during the 1990s, especially due to its relation to the discovery of giant magnetoresistance and its subsequent application to read heads in information storage devices. Besides its huge technological importance, IEC is also a very intriguing phenomenon. Its basic physics can be easily understood in terms of very simple models for the electronic structures of the materials involved, but there are many subtle behaviors that can only be fully accounted for if one employs realistic band structure calculations. Most realistic calculations of IEC in layered systems employ a noninteracting description of the spacer material. While this is certainly appropriate for free-electron-like metals as Cu, Ag, and Au, it is less so for transition metals. Extreme examples would be Pd and Pt which, although nonmagnetic in bulk form, exhibit very large Stoner enhancement. To the best of our knowledge, the influence of Coulomb interaction within the spacer layer on the properties of IEC remains unexplored, except for the work reported in Ref. 9. In it, Takahashi studies the IEC between Fe layers separated by Pd by mapping the interaction onto a classical Heisenberg Hamiltonian and uses the static susceptibility, calculated within the random phase approximation, to estimate the effect of Coulomb interaction in Pd.

Another form of interlayer coupling has gained notoriety in recent years due to seminal works by Slonczewsky[10] and Berger.[11] The idea is that a ferromagnet in contact with a nonmagnetic metallic medium will, when perturbed from its equilibrium configuration, inject a spin current into the medium, that can be absorbed by a second ferromagnet in contact with the same medium.[12] This is very attractive from the technological point of view, since signal transmission by pure spin currents would be much less affected by the dissipation mechanisms that strongly affect charge currents. That said, there are other mechanisms that can influence pure spin currents and one of them is the Coulomb repulsion between electrons within the metallic medium.

In this paper we will present the results of our investigations concerning the effects of Coulomb interaction in Pd on the properties of the "traditional," RKKY-like interlayer exchange coupling and on the dynamical coupling promoted by the emission and absorption of pure spin currents by ferromagnetic films. We employed realistic electronic structure calculations to describe both the ground state and the spin dynamics of layered systems composed of several atomic layers of Co or Ni deposited on Pd substrates. The formalism we used has been described in great detail in previous publications.[13–15,19–21] Thus, in Sec. II we remind the reader of the main features of our theoretical approach and establish the notation that will be used throughout the paper. In Sec. III we present and discuss the results of our numerical calculations, and in Sec. IV we offer our final remarks.

II. THEORETICAL FRAMEWORK

A. Electronic structure and self-consistent ground state

We describe the electronic structure of the system using a multiorbital extension of the Hubbard model,

$$
\begin{aligned}
H = & \sum_{ll'} \sum_{\mu\nu} \sum_{\sigma} t_{ll'}^{\mu\nu} a_{l\mu\sigma}^{\dagger} a_{l'\nu\sigma} \\
& + \sum_{l} \sum_{\sigma\sigma'} \sum_{\mu\nu\mu'\nu'} U_l^{\mu\nu\mu'\nu'} a_{l\mu\sigma}^{\dagger} a_{l\nu\sigma'}^{\dagger} a_{l\nu'\sigma'} a_{l\mu'\sigma} \\
& + \frac{g\mu_B B_z}{2} \sum_{l,\mu} (a_{l\mu\uparrow}^{\dagger} a_{l\mu\uparrow} - a_{l\mu\downarrow}^{\dagger} a_{l\mu\downarrow}),
\end{aligned}
\tag{1}
$$

where $a_{l\mu\sigma}^{\dagger}$ creates an electronic state in atomic orbital μ at lattice site l with spin σ. $t_{ll'}^{\mu\nu}$ are hopping matrix elements extracted from DFT-based calculations and $U_l^{\mu\nu\mu'\nu'}$ are the matrix elements of the effective on-site Coulomb interaction. This model provides magnetizations, local densities of states, and local occupancies in excellent agreement with DFT-based calculations. The last term in Eq. (1) is the Zeeman energy corresponding to a uniform magnetic field of intensity B_z applied to the sample along the z axis. It is essential to the description of ferromagnetic resonance experiments. The constants g and μ_B are the electron's gyromagnetic factor and the Bohr magneton, respectively.

Here we address the self-consistent ground state (SCGS) of ferromagnetic films of Ni or Co adsorbed to Pd substrates. We employed bulk tight-binding parameters to describe the electronic structures of both the magnetic film and Pd substrates. This is not ideal but we believe it is not critical either, since the effects we want to explore are not related to details of the materials' band structures but to a very robust feature of bulk Pd, namely its high Stoner enhancement. In order to determine the SCGS a mean-field approximation is adopted in which the interaction term in Eq. (1) is replaced by

$$
\begin{aligned}
& \sum_{l} \sum_{\mu\in d} \sum_{\sigma} V_l^0 a_{l\mu\sigma}^{\dagger} a_{l\mu\sigma} - \sum_{l} \sum_{\mu\in d} \frac{U_l m}{2} (a_{l\mu\uparrow}^{\dagger} a_{l\mu\uparrow} - a_{l\mu\downarrow}^{\dagger} a_{l\mu\downarrow}) \\
& + \frac{g\mu_B B_z}{2} \sum_{l,\mu} (a_{l\mu\uparrow}^{\dagger} a_{l\mu\uparrow} - a_{l\mu\downarrow}^{\dagger} a_{l\mu\downarrow}).
\end{aligned}
\tag{2}
$$

The on-site potential V_l^0 at each magnetic site is adjusted in order to guarantee local charge neutrality. The fact that the self-consistent mean field depends only on the magnetization is a consequence of the simple form we adopt for the matrix elements of the Coulomb interaction,

$$
U_l^{\mu\nu\mu'\nu'} = U_l \delta_{\mu\nu'} \delta_{\nu\mu'}.
\tag{3}
$$

A more complex parametrization depending on three parameters has been tested in several cases and shown to yield only very small quantitative differences when compared to the much simpler approximation described by Eq. (3).[15]

The famous Stoner criterion for the appearance of local magnetic moments in metals establishes that the ground state of the metal will be spin polarized provided that the product of the effective Coulomb repulsion intensity U by the paramagnetic density of states per spin at the Fermi level $\rho^0(E_F)$ exceeds unity. In the $3d$ transition metals Fe, Co, and Ni the criterion in easily satisfied. In noble metals such as Cu, Au, and Ag, $U\rho^0(E_F)$ is well below 1. In Pd, however, specific heat and uniform spin susceptibility measurements indicate that $U\rho^0(E_F) \sim 0.9$.[22,23] This means that while the ground state of bulk Pd has negligible spin polarization, correlation effects should not be neglected. There is much strong evidence of the importance of correlation effects in Pd, some of which has been mentioned in the introduction. One strong piece of evidence that palladium is on the verge of becoming ferromagnetic is the giant polarization cloud produced by Fe impurities added in very small concentrations to bulk Pd.[25]

We first consider ferromagnetic films of Co or Ni deposited on semi-infinite Pd substrates. We use the values $U_{\text{Pd}} = 0.76$ eV (according to the estimate presented in the previous paragraph) and $U_{\text{Co,Ni}} = 1$ eV.[24] As shown in Fig. 1, the magnetic moments in the substrate are far from negligible, especially within the atomic layers close to the interface. However, it is worth noting that beyond the fifth atomic layer the
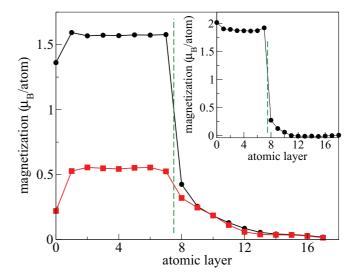

FIG. 1. (Color online) Magnetic moment per atom for 8Co/Pd(001) at each atomic layer from the surface of the Co ultrathin-film (layer 0) to the 10th layer of Pd (layer 17). The green dashed line marks the interface between the ferromagnetic film (Co, black solid circles, and Ni, red solid squares) and the Pd substrate. The inset shows the results of a DFT-based calculation for 8Co/Pd(001).
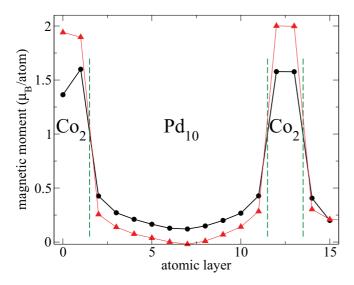
FIG. 2. (Color online) Magnetic moment per atom at each atomic layer of $Co_2/Pd_{10}/Co_2/Pd(001)$ (solid circles). The vertical dashed lines mark the interfaces between Co and Pd. Only the two layers of the substrate closest to the second Co film are shown. The triangles represent the magnetizations obtained from a DFT calculation on the same system [$Co_2/Pd_{10}/Co_2/Pd(001)$].

magnetic moment in the Pd spacer layer becomes negligible ($\lesssim 0.05\mu_B$). For the Ni/Pd(001) system the magnetization of the Pd layer closest to the interface is comparable to the average magnetization of the Ni layers. In Fig. 2 we show the calculated magnetic moments of a $Co_2/Pd_{10}/Co_2$ trilayer deposited on the surface of semi-infinite Pd(001). These results are similar to the ones depicted in Fig. 1.

In order to verify whether the ground-state magnetizations obtained within our tight-binding model are compatible to the predictions of density functional theory we performed an *ab initio* calculation using the VASP package.[26,27] We employed a functional based on the local density approximation (LDA) for exchange-correlation effects.[28] LDA was used because it leads to a better description of the magnetic properties of Pd, compared to generalized gradient approximation calculations.[3] The interaction between the valence electrons and the ionic cores was taken into account by means of the projector augmented wave method (PAW).[29] The single-particle wave functions were expanded in a plane wave basis up to an energy cutoff of 350 eV. To sample the Brillouin zone the Monkhorst-Pack method was used with $12 \times 12 \times 1$ point grids.[30] Large unit cells with vacuum regions $4a_0$ thick were employed in order to simulate the surfaces, where $a_0 = 3.89$ Å is the experimental lattice parameter of Pd.

B. Spin dynamics

The spin dynamics is investigated, within the linear response regime, through the transverse spin susceptibility matrix

$$\chi_{\mu\nu}(\vec{R}_l, \vec{R}_{l'}; t) = -i\theta(t)\langle[S_\mu^+(\vec{R}_l; t), S_\nu^-(\vec{R}_{l'}; 0)]\rangle. \quad (4)$$

μ, ν are orbital indices, $\vec{R}_l$ is the position of lattice site l, $S_\mu^+(\vec{R}_l) = a_{l\mu\uparrow}^\dagger a_{l\mu\downarrow}$, and $S_\mu^-(\vec{R}_l) = [S_\mu^+(\vec{R}_l)]^\dagger$. The equation of motion for $\chi_{\mu\nu}(\vec{R}_l, \vec{R}_{l'}; t)$ is coupled to higher order suscep-

tibilities through terms arising from the effective Coulomb interaction. We utilize a decoupling procedure based on the random phase approximation (RPA).[16]

From the (time) Fourier transform of $\chi_{\mu\nu}(\vec{R}_l, \vec{R}_{l'}; t)$ it is possible to extract the response to transverse magnetic fields and the magnon density of states. For the film geometry it is convenient to work in a mixed basis of Bloch states within each atomic layer and localized states in the direction perpendicular to the layers,

$$|\vec{k}_\parallel; l; \mu\rangle = \frac{1}{N_\parallel}\sum_{\vec{R}_\parallel} e^{i\vec{k}_\parallel \cdot \vec{R}_\parallel}|\vec{R}_\parallel; l; \mu\rangle. \quad (5)$$

$|\vec{R}_\parallel; l; \mu\rangle$ is the state vector associated with an atomic orbital μ at site $\vec{R}_\parallel$ within atomic layer l. For systems with translation symmetry within the atomic layers, the susceptibility defined by Eq. (4) is a function of the relative position in the direction parallel to the atomic layers,

$$\chi_{\mu\nu}(\vec{R}_l, \vec{R}_{l'}; t) = \chi_{\mu\nu}(\vec{R}_\parallel - \vec{R}_\parallel'; l, l'; t). \quad (6)$$

It is most useful to calculate the Fourier transform of Eq. (4) within the atomic layers, together with the Fourier transform from time to frequency (or energy) domain. The object we are interested in is, thus,

$$\chi_{\mu\nu}(\vec{Q}_\parallel; l, l'; \Omega) = \frac{1}{N_\parallel}\sum_{\vec{R}_\parallel} e^{i\vec{Q}_\parallel \cdot \vec{R}_\parallel} \int dt\, e^{i\Omega t}\chi_{\mu\nu}(\vec{R}_\parallel; l, l'; t). \quad (7)$$

It can be easily shown that this is precisely the response function of the system to a magnetic field circularly polarized in the direction perpendicular to the equilibrium magnetization, whose space-time dependence in the direction parallel to the layers is a plane wave with wave vector $\vec{Q}_\parallel$ and frequency $\Omega/\hbar$. The spectral density associated with this transverse susceptibility may also be interpreted as the partial density of states of magnons at layer l with wave vector $\vec{Q}_\parallel$,

$$A_l(\vec{Q}_\parallel; \Omega) = -\frac{1}{\pi}\text{Im}\sum_{\mu\nu}\chi_{\mu\nu}(\vec{Q}_\parallel; l, l; \Omega). \quad (8)$$

From the peaks of $A_l(\vec{Q}_\parallel; \Omega)$ as a function of Ω for fixed values of $\vec{Q}_\parallel$ it is possible to extract the spin wave spectrum of the system. The particular case $\vec{Q}_\parallel = 0$ is especially interesting: It corresponds to the uniform excitation field applied to the sample in ferromagnetic resonance (FMR) experiments. Thus, we can calculate the spin wave spectra and the FMR spectra of ultrathin magnetic films within the same formalism. Moreover, we have information about the spectral intensities on a layer-by-layer basis, which allows us to study nonlocal spin responses with relative ease.[19]

III. RESULTS

A. Spin pumping

We start by analyzing the FMR spectra of several Co and Ni ultrathin films on Pd(001). The FMR linewidth is directly related to the spin current pumped by the ferromagnetic film into the substrate. It has been argued, based on geometric reasoning, that the FMR linewidth should decrease as the

inverse of the ferromagnetic film thickness N, due to the fact that spin pumping is an interface phenomenon. This argument, however, ignores the effects of quantum interferences within the ferromagnetic film and the fact that the electronic structure of the film depends on its thickness. This is especially true for the ultrathin films (1 to ~10 atomic layers thick) we consider here.

When the FMR precession is described phenomenologically through the Landau-Lifshitz-Gilbert equation, as it very frequently is, the effective damping term usually takes the form

$$\alpha \hat{m} \times \frac{d\hat{m}}{dt}, \tag{9}$$

where $\hat{m}$ is a unit vector parallel to the sample's magnetization and α is the Gilbert constant, which embodies the damping due to all possible mechanisms. When spin pumping is the only active damping mechanism, the FMR linewidth $\Delta\Omega$ is proportional to the resonance frequency Ω_0 for small Ω_0. Thus, the spin pumping contribution to the Gilbert parameter α is proportional to the ratio $\Delta\Omega/\Omega_0$ and is independent of Ω_0 for small Zeeman fields. We have chosen this ratio as the measure of spin pumping rate in our calculations.

One virtue of our model calculations is that we can test several contributions to the damping rate separately. Pd has a large Stoner enhancement and, of course, its d bands are crossed by the Fermi energy. Thus we first analyze the damping rate in the absence of electron-electron interaction in Pd. This amounts to making $U_l^{\mu\nu\mu'\nu'} = 0$ in Eq. (1) whenever the value of l corresponds to a Pd site.

The linewidths extracted from FMR calculations using such approach exhibit a clear power-law decrease as a function of N, as shown in Fig. 3. The power-law exponent is ~0.83 for Co and ~0.74 for Ni. Previous calculations for ultrathin Fe films on W,[19] which has negligible Stoner enhancement but whose d bands are crossed by the Fermi energy, also show a power-law exponent close to 0.8. When W was replaced by free-electron-like substrates such as Au and Ag, the exponent
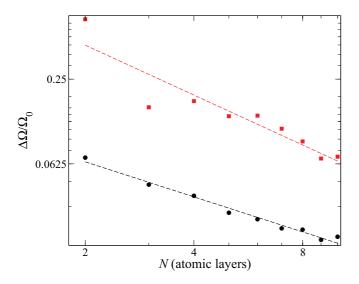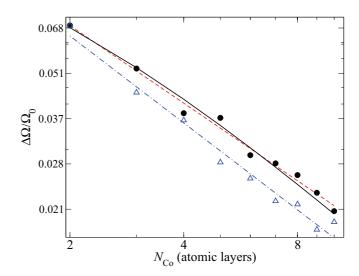

FIG. 4. (Color online) Damping rate for NCo/Pd(001) as a function of the Co film thickness N for interacting Pd (solid circles) and noninteracting Pd (open triangles) substrates. The solid line is a $1/(N + N_0)$ fitting of the results for the enhanced substrate (see text). The (red) dashed line is a $1/N^\alpha$ fitting of the results for the enhanced substrate, with $\alpha \approx 0.74$. The dot-dashed line is a $1/N^\alpha$ fitting of the results for the nonenhanced substrate with $\alpha \approx 0.83$ (also shown in Fig. 3).

came out very close to 1. It is, however, difficult to attribute such deviations to general electronic structure features of the substrate. In fact, as we have just seen, two different magnetic materials on the same substrate can lead to two rather different power-law behaviors.

The effect of Coulomb interaction in Pd on spin pumping can be seen in Fig. 4. The solid circles are linewidth values extracted from FMR spectra calculated for NCo/Pd(001). N has been varied from 1 to 10 and enhancement effects have been taken into account within the first 10 layers of the Pd(001) substrate (beyond the tenth Pd layer the magnetic moment in Pd is virtually zero). We also show two fittings to the linewidth data for comparison: The dashed black line is a Δ_0/N^α fitting and the solid red line is a $\Delta_0/(N + N_0)$ fitting. Δ_0, α, and N_0 have been treated as adjustable parameters. Consider the Δ_0/N^α fitting first: Our results are best fitted to $\alpha \approx 0.7$, which is smaller than the value for a noninteracting Pd substrate by 13%. One way to interpret the effects of the enhancement is to think about the polarization of the substrate as an "effective thickness" added to the magnetic film. In this case the linewidth versus thickness curve should behave like $\Delta_0/(N + N_0)$, our second choice for a fitting. In this particular case we found the best fitting corresponds to $N_0 \approx 1.4$. This suggests that the Pd polarization acts as ~1.4 "effective magnetic layers." Going back to the layer-by-layer distribution of magnetic moments presented in Sec. II A, Fig. 1, we notice that the integrated magnetic moment induced in Pd is ~$1.3\mu_B$, which is close to the average magnetic moment of the Co layers. Of course we did not expect that N_0 would yield a magnetic moment identical to the integrated magnetic moment induced in Pd, but the fact that both quantities are of the same order of magnitude is an indication that our interpretation makes sense. One further piece of evidence in favor of this interpretation is the fact that
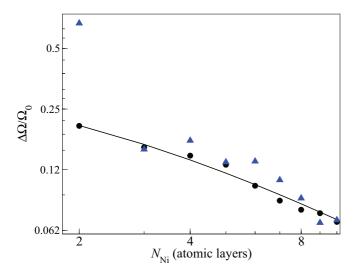

FIG. 3. (Color online) Spin pumping rate for NCo/Pd(001) (solid black circles) and NNi/Pd(001) (solid red squares). The effective Coulomb interaction in Pd has been turned off. The dashed lines are fittings to power laws $N^{-\alpha}$ with exponents $\alpha_{Co} \sim 0.83$ and $\alpha_{Ni} \sim 1.2$.

FIG. 5. (Color online) Damping rate for NNi/Pd(001) as a function of the Ni film thickness N for interacting Pd (solid circles) and noninteracting Pd (solid triangles) substrates. The solid curve is a $1/(N + N_0)$ fitting of the results for the enhanced substrate (solid circles).

we find the effective thickness for Ni $N_0 \approx 2.2$ (see Fig. 5). Since the magnetic moments of the Ni films are smaller than those of Co films, and the polarization of the underlying Pd is very similar in both cases, its role as an effective thickness is more pronounced in Ni.

We show in the same figure the linewidths with electron-electron interaction turned off in Pd, previously presented in Fig. 3. Notice that there is an overall increase in linewidth when the electron-electron interaction is turned on in the Pd substrate. This may be due to an increase in the interface transmissivity. Turning on Coulomb repulsion in the Pd substrate causes an exchange splitting between the majority and minority spin subbands of the Pd layers close to the interface. This splitting decreases smoothly as one goes into the substrate, increasing the effective transmission coefficient of the interface. The effect is analogous to the smoothing of a potential step. A large interface transmissivity means a larger spin current pumped into the substrate and a larger damping rate to the FMR precession. It is also interesting to notice that the linewidth dependence on the Co thickness has a nonnegligible oscillatory component, which may be attributed to quantum interference effects.

The spin pumping rate for Ni films on Pd has a more complex behavior than for Co films, as can be seen in Fig. 5. With $U_{Pd} = 0$ it displays strong oscillations as a function of N. While it is difficult to extract the rate of decay from a strongly oscillatory function with so few points, a $1/N$ curve fits reasonably well our results. When electron-electron interaction is turned on in Pd the strong oscillations are partially suppressed and, as stated in the previous paragraph, the results are well fitted to a $1/(N + N_0)$ curve (the solid curve in Fig. 5).

B. Interlayer exchange coupling through Pd

There are many ways to estimate the magnitude of the exchange coupling between magnetic entities separated by nonmagnetic metals.[31] One widely used approach, that can be implemented in various forms, is to calculate energy differences between ferromagnetic and antiferromagnetic configurations. A more subtle approach is to calculate the total energy variation due to small deviations from either ferromagnetic or antiferromagnetic configurations.[32] This is what we refer to as the "static" exchange coupling. Both approaches rely on the assumption that the magnetic moments carried by the magnetic entities may be treated as macrospins and their energy can be expressed as a function of their relative orientation.

There is one way to estimate the exchange interaction energy between magnetic moments that is identical in principle to the experimental determination of IEC using ferromagnetic resonance experiments. Once the magnetic moments are perturbed from their equilibrium configuration their precessional motion can be decomposed into normal modes, from which it is possible to extract the intensity of the interaction between them.[19] It is simple to show, for example, that two magnetic moments interacting via a Heisenberg-like term will have two normal modes, one in-phase (the so-called acoustic mode) and one 180° out of phase (the "optical" mode). The difference between the energies of these two modes is proportional to the strength of the coupling between the spins. This approach to infer the strength of the exchange coupling has been used several times, both theoretically[19] and experimentally.[17,18] In Ref. 19 we discussed the relationship between the acoustic mode-optical mode splitting and the IEC. Figure 6 of that reference shows a numerical comparison between the IEC calculated by an adiabatic method and the values of the optical mode-acoustic mode splitting. For a normal-metal spacer such as Cu both methods are seen to agree very well with each other.

Thus, based on the preceding discussion, to investigate the effects of Coulomb repulsion on the IEC between magnetic ultrathin films separated by Pd we calculated the FMR spectra of trilayers formed by two ferromagnetic layers separated by a Pd slab. We then extracted the optical mode-acoustic mode splitting $J \equiv \Omega_{opt} - \Omega_{ac}$ and use it as a measure of the IEC between the ferromagnetic layers. The results of our calculations are presented in Figs. 6 and 7. We only investigated relatively small Pd thicknesses because these calculations are extremely demanding computationally for thick spacers. In Fig. 6 we present J for two Co films separated by an N-atomic-layers-thick Pd spacer where the effective Coulomb interaction is active. Even in this pre-asymptotic region of relatively small spacer thicknesses it is expected that the exchange coupling mediated by an independent electron system (for instance, typical nonmagnetic metals) would display an oscillatory behavior. Our results indicate that the oscillations are suppressed by the Coulomb interaction between d electrons in Pd. To confirm that this is not simply a special feature of the electronic structure of Pd we repeated the calculations with the same electronic structure but with the Coulomb repulsion turned off in all Pd layers. These results are shown in the inset of Fig. 6. Two differences are readily noticed: In the case where $U_{Pd} = 0$ the exchange coupling is one order of magnitude smaller and there are clear oscillations. Similar behavior has been observed experimentally in Fe(001)/Pd(001)/Fe(001) multilayers.[33] The suppression of
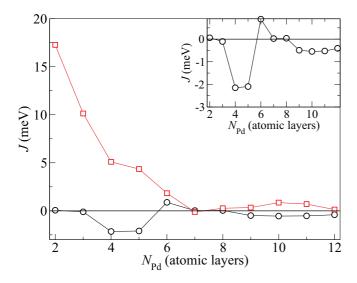
FIG. 6. (Color online) Interlayer exchange coupling between two Co films (with two atomic layers each) separated by N_{Pd} Pd atomic layers measured by the frequency of the optical FMR mode (squares). For comparison we show the same IEC calculated without exchange enhancement within the Pd spacer (open circles). For clarity, due to the magnitude mismatch between the two results, we repeat the IEC with the Coulomb repulsion turned off in Pd and show the results in the inset.

the oscillatory behavior is the most striking qualitative feature of the experimental results.

For Ni films there is a substantial change in the exchange coupling due to Coulomb repulsion for small Pd thicknesses, as seen in Fig. 7. At large distances, however, the coupling seems to be little affected by the Coulomb interaction within the Pd substrate. It is also interesting that the strength of the exchange coupling is considerably larger between Ni films than between Co films when the Coulomb repulsion is turned off in the Pd spacer layer. This may be due to the large spin polarizability of Pd even when $U_{Pd} = 0$. Since the magnetic

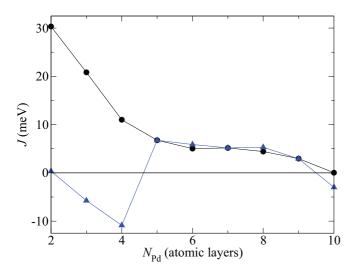
FIG. 7. (Color online) Frequency of the optical (out-of-phase) precession mode of two Ni films (with two atomic layers each) separated by N_{Pd} atomic layers.

moment of Ni is much smaller than that of Co, even the small polarization of nonenhanced Pd is enough to affect the exchange coupling at large distances. Notice that at short distances the exchange coupling between Ni layers when $U_{Pd} = 0$ would be antiferromagnetic. When we take Coulomb repulsion within Pd into account the situation changes dramatically, since Pd polarization follows the neighboring Ni magnetic moments and nearest-neighbor Pd-Pd exchange coupling is ferromagnetic. At large distances there is a relatively thick layer of Pd with very small magnetic moment in between the polarized Pd layers, which results in an effective system similar to the nonenhanced Pd spacer sandwiched by Ni films.

C. Dynamic exchange coupling through Pd

The "static" interlayer exchange coupling between magnetic units A and B embedded into a nonmagnetic metal is often interpreted in terms of the interaction between the magnetic moment of unit A and the spin polarization of the nonmagnetic medium surrounding A produced by unit B and vice versa. The IEC decreases as a power law of the distance d between A and B. For the layered geometry the decay is proportional to d^{-2}. Thus, when layers A and B are sufficiently far apart, the IEC is negligible and the optical mode–acoustic mode splitting observed in the FMR spectrum for coupled layers vanishes. Nevertheless, if the magnetization of layer B is perturbed by a time-dependent transverse field, the magnetization of layer A also acquires a time-dependent transverse component.[17,19–21] This "dynamic coupling" between the magnetizations of units A and B may be viewed as a consequence of the spin current pumped by the out-of-equilibrium magnetizations of A and B.[12] Of course, if the distance between A and B is such that there is still some "static" coupling between them, a contribution from the time-dependent polarization of the intervening electron gas will also be present, in addition to that of the spin current.

One way to measure the intensity of the dynamic coupling is through the nonlocal susceptibility χ_{AB}, where A and B represent two distinct magnetic unities. Schematically, if a transverse magnetic field $h_B^{\perp}$ is applied to unit B, $\chi_{AB} h_B^{\perp}$ is the transverse component acquired by the magnetization of unit A. Since the number of spacer layers may affect also the local response χ_{AA} we chose the ratio $|\chi_{AB}|/|\chi_{AA}|$ as a measure of the dynamic coupling between films A and B. Of course this ratio is wave-vector and frequency dependent. In FMR experiments, however, the exciting field is usually uniform in the direction parallel to the sample's surface, so it is natural to choose $\vec{Q}_{\parallel} = 0$. One would also like to maximize the effect, so the resonance frequency for the uniform mode should be chosen. With these considerations in mind we defined our measure of the dynamic coupling between layers A and B as

$$J^{dyn} \equiv \frac{\left|\chi_{AB}\left(\vec{Q}_{\parallel} = 0, \Omega_0^{ac}\right)\right|}{\left|\chi_{AA}\left(\vec{Q}_{\parallel} = 0, \Omega_0^{ac}\right)\right|}. \tag{10}$$

We calculated the dynamic coupling between two Co films separated by Pd layers with varying thickness N_{Pd} using Eq. (10) above. The results are shown in Fig. 8. To assess the effect of Coulomb interaction in Pd we performed calculations in which the effective Coulomb interaction was set to zero
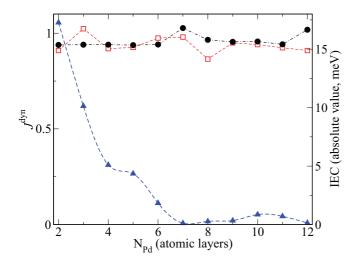
FIG. 8. (Color online) Dynamic coupling between two Co films (with two atomic layers each) separated by N_{Pd} atomic layers. The results represented by solid circles where obtained with Coulomb repulsion turned off within the Pd spacer. The dashed and dot-dashed lines are meant as guides to the eye only. The absolute value of the static IEC (solid triangles) is also shown for comparison (scale on the right).

within the Pd spacer layer (open squares in Fig. 8). The dynamic coupling with the Coulomb repulsion turned off in Pd oscillates as a function of N_{Pd} with a constant amplitude. When the Coulomb repulsion is turned on the oscillations are suppressed for $N_{Pd} \leqslant 6$. For such thicknessess the whole Pd spacer is strongly spin polarized. For $N_{Pd} > 6$ there are atomic planes of Pd with negligible polarization close to the center of the spacer layer, which restore the oscillatory behavior of the dynamic coupling.

It is also interesting to remind ourselves about the behavior of the static IEC we calculated previously. We plot the static IEC as solid triangles in Fig. 8. Notice that it decays relatively fast with N_{Pd}, being very close to zero for $N_{Pd} \geqslant 7$, whereas the dynamic coupling is clearly finite for the entire range of N_{Pd} considered. In fact, the range of the dynamic coupling is infinite within our model, since we do not consider any mechanism that could dissipate the spin current emitted by the pumped Co film. This is equivalent to saying that the range of the dynamic coupling should only be limited by the spin diffusion length.

The above discussion about the infinite range of dynamic coupling applies to cases where the pumping field is uniform in the direction parallel to the ferromagnetic layers. In that case the precession mode being excited is the uniform ($\vec{Q}_\parallel = 0$) mode and rotation symmetry in spin space prohibits decaying of this mode into uncorrelated electron-hole pairs (the so-called Stoner excitations). If, however, the pumping field has a finite wave vector, decaying of the spin wave into Stoner excitations is allowed and the dynamic coupling should acquire a finite range as a function of N_{Pd}. This decaying is shown clearly in Fig. 9, which depicts results for the dynamic coupling J^{dyn} calculated for a finite wave vector $\vec{Q}_\parallel = \frac{0.44}{a_0}\hat{\imath}$. As above, we present results in the absence of Coulomb interaction in Pd (open circles) for comparison. The decaying is relatively slow for small Pd thicknesses, indicating that the strong polarization
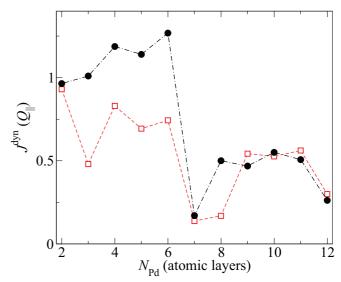

FIG. 9. (Color online) Dynamic coupling between two Co films (with two atomic layers each) separated by N_{Pd} atomic layers for a finite wave vector of the pumping field, $\vec{Q}_\parallel = \frac{0.44}{a_0}\hat{\imath}$. The results represented by solid circles where obtained with Coulomb interaction turned off within the Pd spacer. The dashed and dot-dashed lines are meant as guides to the eye only.

of the substrate suppresses partially the decaying into Stoner modes. This is expected since spin polarization reduces the density of Stoner modes.

IV. CONCLUDING REMARKS

We have investigated the influence of an effective Coulomb interaction within d orbitals on spin pumping and exchange coupling, dynamic and static, through Pd substrates. We used realistic models to describe the electronic structures of both magnetic films and substrate. Our formalism to study spin pumping and interlayer exchange coupling, static and dynamic, is based on the calculation of the dynamic response of the system to time-dependent magnetic fields transverse to the equilibrium direction of the system's magnetization. We found that Coulomb interaction within the Pd layers has a small but nonnegligible effect on the spin pumping rate at zero transverse wave vector and without spin-orbit coupling. However, Coulomb interaction within Pd can strongly affect the behavior of IEC between Co and Ni films: It suppresses the oscillations of the IEC as a function of spacer thickness, and increases substantially the strength of the IEC. The Coulomb interaction within Pd also suppresses the oscillations of the dynamic interlayer coupling both at zero wave vector. Nevertheless, the effects are much more pronounced for small Pd thicknesses, due to the strong polarization of all Pd spacer layers. Investigations of the combined effect of Coulomb interaction and spin-orbit coupling are underway.

*antc@if.uff.br

[1] P. Lederer and D. L. Mills, Phys. Rev. **165**, 837 (1968).

[2] R. Doubble, S. M. Hayden, P. Dai, H. A. Mook, J. R. Thompson, and C. D. Frost, Phys. Rev. Lett. **105**, 027207 (2010).

[3] S. S. Alexandre, M. Mattesini, J. M. Soler, and F. Yndurain, Phys. Rev. Lett. **96**, 079701 (2006).

[4] A. T. Costa, R. B. Muniz, S. Lounis, A. B. Klautau, and D. L. Mills, Phys. Rev. B **82**, 014428 (2010).

[5] K. Zakeri, Y. Zhang, J. Prokop, T.-H. Chuang, N. Sakr, W. X. Tang, and J. Kirschner, Phys. Rev. Lett. **104**, 137203 (2010).

[6] A. A. Khajetoorians, S. Lounis, B. Chilian, A. T. Costa, L. Zhou, D. L. Mills, J. Wiebe, and R. Wiesendanger, Phys. Rev. Lett. **106**, 037205 (2011).

[7] B. Chilian, A. A. Khajetoorians, S. Lounis, A. T. Costa, D. L. Mills, J. Wiebe, and R. Wiesendanger, Phys. Rev. B **84**, 212401 (2011).

[8] J. Foros, G. Woltersdorf, B. Heinrich, and A. Brataas, J. Appl. Phys. **97**, 10A714 (2005).

[9] Y. Takahashi, Phys. Rev. B **56**, 8175 (1997).

[10] J. Slonczewski, J. Magn. Magn. Mater. **195**, L261 (1999).

[11] L. Berger, Phys. Rev. B **54**, 9353 (1996).

[12] Y. Tserkovnyak, A. Brataas, G. E. W. Bauer, and B. I. Halperin, Rev. Mod. Phys. **77**, 1375 (2005).

[13] L. H. M. Barbosa, R. B. Muniz, A. T. Costa, and J. Mathon, Phys. Rev. B **63**, 174401 (2001).

[14] A. T. Costa, R. B. Muniz, and D. L. Mills, Phys. Rev. B **68**, 224435 (2003).

[15] R. B. Muniz and D. L. Mills, Phys. Rev. B **66**, 174417 (2002).

[16] G. F. Giuliani and G. Vignale, *Quantum Theory of the Electron Liquid* (Cambridge University Press, Cambridge, 2005), p. 196.

[17] K. Lenz, T. Tolinski, J. Lindner, E. Kosubek, and K. Baberschke, Phys. Rev. B **69**, 144422 (2004).

[18] Z. Celinski and B. Heinrich, J. Magn. Magn. Mater. **99**, L25 (1991).

[19] A. T. Costa, R. B. Muniz, and D. L. Mills, Phys. Rev. B **73**, 054426 (2006).

[20] A. T. Costa, R. B. Muniz, M. S. Ferreira, and D. L. Mills, Phys. Rev. B **78**, 214403 (2008).

[21] A. T. Costa, R. B. Muniz, and M. S. Ferreira, New J. Phys. **10**, 063008 (2008).

[22] B. Giovannini, M. Peter, and J. R. Schrieffer, Phys. Rev. Lett. **12**, 736 (1964).

[23] S. Doniach and S. Engelsberg, Phys. Rev. Lett. **17**, 750 (1966).

[24] F. J. Himpsel, J. Magn. Magn. Mater. **102**, 261 (1991).

[25] G. G. Low and T. M. Holden, Proc. Phys. Soc. **89**, 119 (1966).

[26] G. Kresse and J. Hafner, Phys. Rev. B **49**, 14251 (1994).

[27] G. Kresse and J. Furthmüller, Comput. Mater. Sci. **6**, 15 (1996).

[28] J. P. Perdew and A. Zunger, Phys. Rev. B **23**, 5048 (1981).

[29] G. Kresse and D. Joubert, Phys. Rev. B **59**, 1758 (1999).

[30] H. J. Monkhorst and J. D. Pack, Phys. Rev. B **13**, 5188 (1976).

[31] M. Stiles, J. Magn. Magn. Mater. **200**, 322 (1999).

[32] A. Liechtenstein, M. Katsnelson, V. Antropov, and V. Gubanov, J. Magn. Magn. Mater. **67**, 65 (1987).

[33] Z. Celinski, B. Heinrich, J. F. Cochran, W. B. Muir, A. S. Arrott, and J. Kirschner, Phys. Rev. Lett. **65**, 1156 (1990).